Convex Super-resolution Detection of Lines in Images: Supplementary Material

Kévin Polisano*, Laurent Condat†, Marianne Clausel* and Valérie Perrier*

*Univ. Grenoble Alpes, Laboratoire Jean Kuntzmann, F-38000, Grenoble, France
Email: Kevin.Polisano@imag.fr
†Univ. Grenoble Alpes, GIPSA-lab, F-38000, Grenoble, France
Email: Laurent.Condat@gipsa-lab.grenoble-inp.fr

I. Notations explained on a diagram

Recall that,

$$u^\sharp = s^\sharp * \phi_1 : (t_1, t_2) \in \mathbb{P} \mapsto \sum_{k=1}^{K} \frac{\alpha_k}{\cos(\theta_k)} \varphi_1\Big(t_1 + \tan(\theta_k) t_2 + \frac{\gamma_k}{\cos(\theta_k)}\Big). \tag{1}$$

Since φ_1 is periodic and bandlimited, it is determined by W degrees of freedom only. That is, there exist coefficients $g[n]$, $n = 0, \dots, W-1$, such that φ_1 is a linear combination of shifted Dirichlet kernels:

$$\varphi_1(t_1) = \sum_{n=0}^{W-1} g[n] \frac{\sin\big(\pi(t_1 - n)\big)}{W \sin\big(\pi(t_1 - n)/W\big)}, \quad \forall t_1 \in \mathbb{R}. \tag{2}$$

This is a corollary of the Nyquist-Whittaker-Shannon interpolation theorem.

Let be two convolutions functions φ_1 and φ_2 satisfying assumptions described in the paper, then the discrete filter associated g and h can be used to perform exact convolutions. Given K lines with parameters $(\theta_k, \gamma_k, \alpha_k)$, one can generated the image $v^\sharp$ by formula (1) and (2).

The Fig. 1 illustrates the relation between all continuous and discrete variables. Our goal is to recover the parameters $(\theta_k, \gamma_k, \alpha_k)$ from the degraded image y, by performing the minimization algorithm in the Fourier domain, that is on the bottom line of Fig. 1.

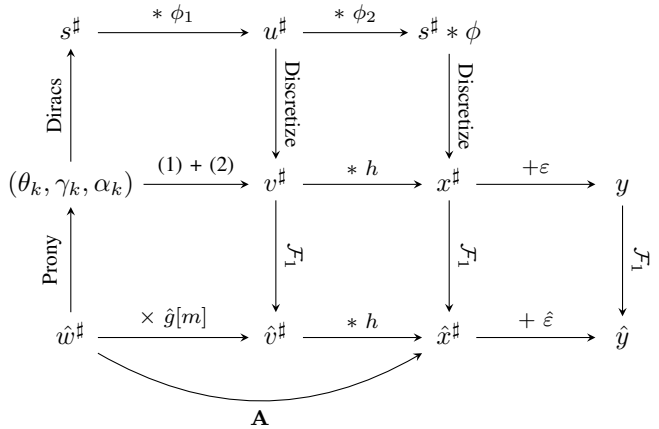

Fig. 1: Relation between variables.

II. SEMIDEFINITE PROGRAM

Proposition 1: The atomic norm

$$\|x\|_{\mathcal{A}} = \inf\left\{\sum_{k=1}^{K} c_k : x = \sum_{k=1}^{K} c_k a(f_k, \phi_k), K \leqslant N\right\}$$

can be characterized by the following semidefinite program:

$$\|x\|_{\mathcal{A}} = \min_{u\in\mathbb{C}^n, u_0 \geqslant 0} \left\{u_0 : \begin{bmatrix} \mathbf{T}(u) & x \\ x^* & u_0 \end{bmatrix} \succcurlyeq 0\right\}. \tag{3}$$

Proof:
Denote the right-hand side of (3) by $SDP(x)$.

• Suppose $x = \sum_{k=1}^{K} c_k a(f_k, \phi_k)$ with $c_k > 0$.
Defining $u = \sum_{k=1}^{K} c_k a(f_k)$, then $u_0 = \sum_{k=1}^{K} c_k$. The atoms are $[a(f_k)]_j = e^{i2\pi f_k j}$, hence

$$\begin{aligned}
\mathbf{T}(a(f_k)) &= \begin{bmatrix} 1 & e^{-i2\pi f_k} & \dots & e^{-i2\pi f_k(N-1)} \\ e^{i2\pi f_k} & 1 & \dots & e^{-i2\pi f_k(N-2)} \\ \vdots & \vdots & \ddots & \vdots \\ e^{i2\pi f_k(N-1)} & e^{i2\pi f_k(N-2)} & \dots & 1 \end{bmatrix} && (4)\\
&= \begin{bmatrix} 1 \\ e^{i2\pi f_k} \\ \vdots \\ e^{i2\pi f_k(N-1)} \end{bmatrix} \begin{bmatrix} 1 & e^{-i2\pi f_k} & \dots & e^{-i2\pi f_k(N-1)} \end{bmatrix} && (5)\\
&= a(f_k)a(f_k)^* && (6)
\end{aligned}$$

We deduce that

$$\begin{aligned}
T(u) &= \sum_{k=1}^{K} c_k \mathbf{T}(a(f_k)) && (7)\\
&= \sum_{k=1}^{K} c_k a(f_k)a(f_k)^* && (8)\\
&= \sum_{k=1}^{K} c_k a(f_k, \phi_k)a(f_k, \phi_k)^* && (9)
\end{aligned}$$

Therefore, the matrix

$$\begin{bmatrix} \mathbf{T}(u) & x \\ x^* & u_0 \end{bmatrix} = \sum_{k=1}^{K} \begin{bmatrix} a(f_k, \phi_k) \\ 1 \end{bmatrix} \begin{bmatrix} a(f_k, \phi_k) \\ 1 \end{bmatrix}^*$$

is positive semidefinite. Given $u_0 = \sum_{k=1}^{K} c_k$, we get $SDP(x) \leqslant \sum_{k=1}^{K} c_k$.
Since this holds for any decomposition of x, we conclude that $SDP(x) \leqslant \|x\|_{\mathcal{A}}$.

• Conversely, let $u \in \mathbb{C}^n$ a vector such that $u_0 \geqslant 0$ and $\begin{bmatrix} \mathbf{T}(u) & x \\ x^* & u_0 \end{bmatrix} \succcurlyeq 0$. In particular we have $\mathbf{T}(u) \succcurlyeq 0$.
The Caratheodory theorem insures that $P \succcurlyeq 0$ if and only if it exists a vector $v \in \mathbb{C}^n$ such that

$$v = \sum_{k=1}^{r} d_k a(f_k)$$

with $r \leqslant N$, $d_k > 0$, distincts f_k, $r = \text{rank}(P)$ and $P = \mathbf{T}(v)$.

We apply this theorem to $P = \mathbf{T}(u)$.

Let denote matrices $D = \text{diag}[d_1, \ldots, d_r]$ and

$$V = \begin{bmatrix} a(f_1) & \cdots & a(f_r) \end{bmatrix} = \begin{bmatrix} 1 & 1 & \cdots & 1 \\ e^{i2\pi f_1} & e^{i2\pi f_2} & \ldots & e^{i2\pi f_r} \\ e^{i2\pi f_1 2} & e^{i2\pi f_2 2} & \ldots & e^{i2\pi f_r 2} \\ \vdots & \vdots & \vdots & \vdots \\ e^{i2\pi f_1 (N-1)} & e^{i2\pi f_2 (N-1)} & \ldots & e^{i2\pi f_r (N-1)} \end{bmatrix}$$

By linearity of the operator $\mathbf{T}$:

$$\begin{aligned} \mathbf{T}(v) &= \sum_{k=1}^{r} d_k \mathbf{T}(a(f_k)) && (12) \\ &= \sum_{k=1}^{r} d_k a(f_k) a(f_k)^* && (13) \\ &= VDV^* && (14) \end{aligned}$$

Since $\mathbf{T}(a(f_k))$ contains only ones on the diagonal, we have $\frac{1}{N}\text{Tr}(\mathbf{T}(v)) = \sum_{k=1}^{r} d_k > 0$. Besides, $\frac{1}{N}\text{Tr}(\mathbf{T}(u)) = u_0$ and $\mathbf{T}(u) = \mathbf{T}(v)$, therefore $u_0 > 0$.

Let be M a general block matrix $M = \begin{bmatrix} A & B \\ B^T & C \end{bmatrix}$, the Schur complement gives

$$[C \succ 0 \Rightarrow M \succcurlyeq 0] \Rightarrow [A - BC^{-1}B^T \succcurlyeq 0]$$

We apply this lemma to $M = \begin{bmatrix} \mathbf{T}(u) & x \\ x^* & u_0 \end{bmatrix}$, with $A = \mathbf{T}(u)$, $B = x$ and $C = u_0$. The left term is verified by hypothesis, hence

$$\mathbf{T}(u) - u_0^{-1} x x^* \succcurlyeq 0 \Leftrightarrow VDV^* - u_0^{-1} x x^* \succcurlyeq 0$$

We define the square matrix V_r by extracting the r first rows of V, which is a Vandermonde matrix, whose determinant is $\det(V_r) = \prod_{1 \leqslant i < j \leqslant r} (f_j - f_i)$. Since we assumed $f_i \neq f_j$, V_r is invertible, and $\text{rank}(V) = r$. Let define $v : \mathbb{C}^r \to \mathbb{C}^N$ and $v^* : \mathbb{C}^N \to \mathbb{C}^r$ the endomorphisms corresponding to matrices V and V^*. We have $\text{rank}(v^*) = \text{rank}(v) = r$. By the rank-nullity theorem:

$$\text{rank}(v^*) + \dim(\text{Ker } v^*) = \dim(\mathbb{C}^N) \Rightarrow \dim(\text{Ker} v^*) = N - r$$

Thus, it exists a vector $p \in \mathbb{C}^N$ such that $V^* p = 0 \Leftrightarrow p^* V = 0$.

Consequently,

$$\begin{aligned} p^*(VDV^* - u_0^{-1} x x^*) p \geqslant 0 &\Leftrightarrow (p^*V) D (V^* p) - u_0^{-1} p^* x x^* p \geqslant 0 && (15) \\ &\Leftrightarrow u_0^{-1} \|p^* x\|_2^2 \leqslant 0 && (16) \\ &\Leftrightarrow \|p^* x\|_2^2 = 0 && (17) \\ &\Leftrightarrow p^* x = 0 && (18) \\ &\Leftrightarrow p \perp x = 0 && (19) \end{aligned}$$

Since $p \in \text{Ker } v^*$, then $x \in (\text{Ker } v^*)^\perp = \text{Im } v$, so it exists a vector $w \in \mathbb{C}^r$ such that $x = Vw = \sum_{k=1}^{r} w_k a(f_k)$, hence

$$VDV^* - u_0^{-1} V w w^* V^* \succcurlyeq 0$$

Besides, $\text{Im } v^* \subset \mathbb{C}^r$ and $\dim(\text{Im } v^*) = \text{rank}(r) = r = \dim(\mathbb{C}^r)$, thus $\text{Im } v^* = \mathbb{C}^r$ and v^* is surjective. Consequently, it exists a vector $q \in \mathbb{C}^N$ such that $V^* q = \text{sign}(w) = \begin{bmatrix} w_1/|w_1| & \cdots & w_r/|w_r| \end{bmatrix}^T$, and

$$q^*(VDV^* - u_0^{-1}Vww^*V^*)q \geqslant 0 \quad \Leftrightarrow \quad (q^*V)D(V^*q) - u_0^{-1}(p^*V)ww^*(V^*p) \geqslant 0 \tag{20}$$

$$\Leftrightarrow \quad \text{sign}(w)^*D\text{sign}(w) - u_0^{-1}\text{sign}(w)^*ww^*\text{sign}(w) \geqslant 0 \tag{21}$$

$$\Leftrightarrow \quad \sum_{k=1}^{r} d_k \left|\frac{w_k}{|w_k|}\right|^2 - u_0^{-1}\left(\sum_{k=1}^{r}\frac{\bar{w_k}}{|w_k|}w_k\right)^2 \geqslant 0 \tag{22}$$

$$\Leftrightarrow \quad u_0^2 \geqslant \left(\sum_{k=1}^{r}|w_k|\right)^2 \tag{23}$$

$$\Leftrightarrow \quad u_0 \geqslant \sum_{k=1}^{r}|w_k| \geqslant \|x\|_{\mathcal{A}} \tag{24}$$

Taking the infimum leads to $SDP(x) \geqslant \|x\|_{\mathcal{A}}$. ■

III. Second version : relaxation of the Chambolle-Pock algorithm

We can also considered the optimization problem as a relaxed version of the Chambolle-Pock algorithm:

$$X^\star = \underset{X\in\mathcal{H}}{\arg\min}\left\{G(X) + \mathbf{H}(\mathbf{L}(X))\right\}, \tag{25}$$

with $G = \frac{1}{2}\|\mathbf{A}\cdot - \hat{y}_r\|^2_{\mathcal{W}}$ which is proximable, $\mathbf{H}x = \sum_{i=0}^{N} H_i x_i$ with $H_i = \iota_{\mathcal{C}}$ and $L_i \in \{L_1^m, L_2^{n_2}\}$ for $i < N$, $H_N = \iota_{\mathcal{B}}$ and $L_N = \text{Id}$. Since we have

$$p = \text{prox}_{\tau G}(\hat{w}_r) \Leftrightarrow \hat{w}_r - p = \nabla(\tau G)(p) \Leftrightarrow \hat{w}_r - p = \tau A^\star(Ap - \hat{y}_r) \Leftrightarrow \hat{w}_r + \tau A^\star\hat{y}_r = (\text{Id} + \tau A^\star A)p$$

then the proximal operator has the following expression:

$$\text{prox}_{\tau G}(\hat{w}_r) = (\text{Id} + \tau\mathbf{A}^*\mathbf{A})^{-1}(\hat{w}_r + \tau\mathbf{A}^\star\hat{y}_r). \tag{26}$$

The operator $\mathbf{A}$ acts on vectors $\hat{w}_m$. Let be A_h the matrix corresponding to the convolution by the filter h. Then, for each $m = 0, \ldots, M$, we have $(\text{Id} + \tau\mathbf{A}^*\mathbf{A})\hat{w}_m = (\text{Id} + \tau|\hat{g}[m]|^2 A_h^* A_h)\hat{w}_m$, whose we are able to compute and store these $M+1$ inverse matrix. We recover Algorithm 1 with $F = 0$. Since $\beta = 0$, we have no restriction on τ, and $\delta = 2$. We deduce that $\sigma = 1/(\tau\mu)$. These relaxed conditions enable to speed up the algorithm process.

IV. The Hough and Radon transforms applied on lines detection

A. Hough transform

The Hough transform tackles the problem of detecting straight lines, in a way consisting to convert this problem into peaks detection in a parameter space. The transformation is done on a binary image, generally obtained after processing the original image by an edge detector. In our case, dealing with blurred image, this pre-processing is not relevant since the lines have some width. Thus, in order to convert the image to a binary one, we apply a certain threshold. We suggest these two possibilities:

- By calling the matlab routine IM2BW.

This will apply a threshold on luminance of the image. We obtain the image Fig. 2 (a), on which we perform the Hough transform, the resulting image is displayed on Fig. 2 (b). The peaks detection (in green), and so the lines estimation (Fig. 2 (c)), altogether fail, due to some artifacts, which have been considered by Errors, Xiaodong Tao and Alwyn Eades, who propose in their article "Errors, Artifacts and Improvements in EBSD Processing and Mapping" a method to remove these artifacts. Nevertheless, as you can seen on Fig. 2 (b), the peaks are in any case spread out because of the binary line's width, which provides a very coarse estimation of the parameters.

- By applying manually a threshold on the pixel values.

This will keep the pixel greater than the threshold at stake. For instance, for a threshold of 230, we obtain the image Fig. 3 (a). The peaks detection is now working, and the lines estimations seems to be correct. This method provides an estimation with a mean error of 10^{-2} for θ_k, and 10^{-1} for γ_k, which is not significantly improved by decreasing the discretization steps of the process. Remark that this method cannot be applied if the lines have different amplitude values, because of the threshold. For the same reason, it is not relevant for image with a large amount of blur or noise.

Therefore, we turned toward the Radon transform, which appears to be more adapted for our topic.

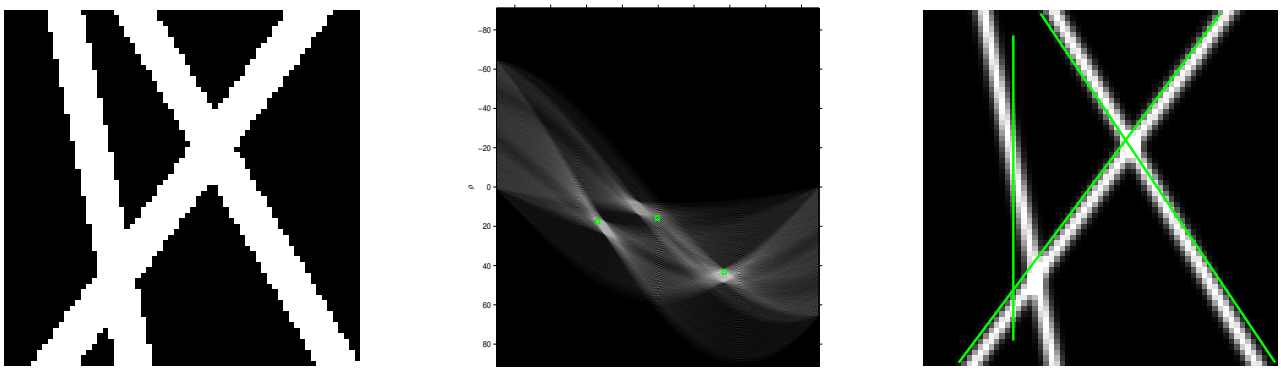

(a) (b) (c)

Fig. 2: (a) The binary version of $x^\sharp$, (b) the corresponding Hough transform with the estimaed peaks, (c) the estimated lines

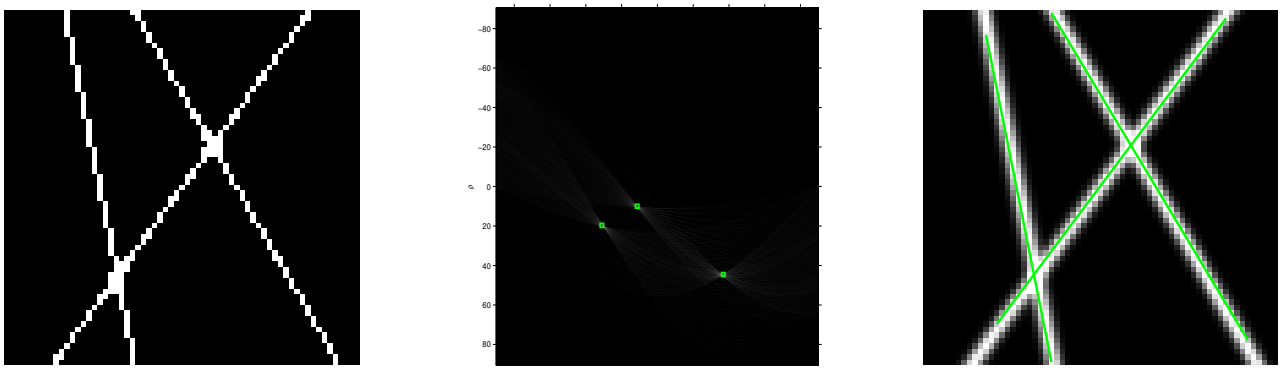

(a) (b) (c)

Fig. 3: (a) The thresholded version of $x^\sharp$, (b) the corresponding Hough transform with the estimaed peaks, (c) the estimated lines

B. Radon transform

The Hough transform is actually related to the famous Radon transform, as a kind of discretization of the latter. The Radon transform can be done directly on grayscale images, and the peaks seem to be less spread than the peaks from the Hough transform, as we can see on Fig. 4 (a). This approach has the advantage to achieve the same mean error of 10^{-1} for γ_k, and a better rate of 10^{-3} for θ_k. Notice that even by decreasing the discretization steps of the process, we rapidly reach a plateau, as illustrated by Fig. 5. Besides, the Radon transform is robust to noise, the peaks remain well detected, as you can observe on Fig. 4 (b). However, this method fail for a large blur, such as presented in the third experiment, the peeks are not clearly recognizable anymore, as you observe on Fig. 4 (c).

To sum up, the Radon transform is more suitable than the Hough transform for detecting lines in a degraded image. But, in both cases, they come up against a discrete limit as soon as we are looking for a greater accuracy. In contrary, our super-resolution method enables to achieve an infinite precision for line's parameters.

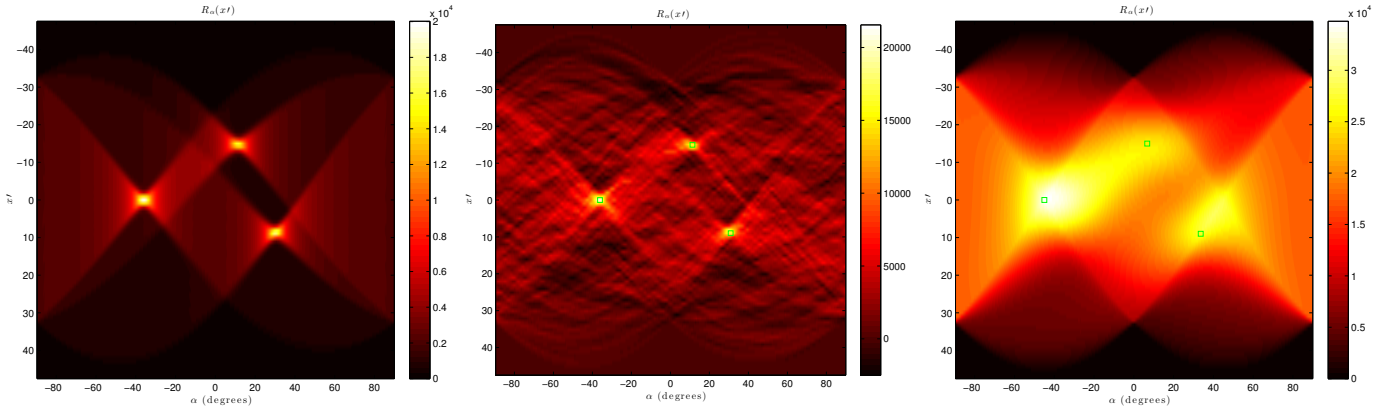

(a) (b) (c)

Fig. 4: The Radon transform of the image y for experiment 1, 2 and 3. The theoretical parameters of lines are in green.

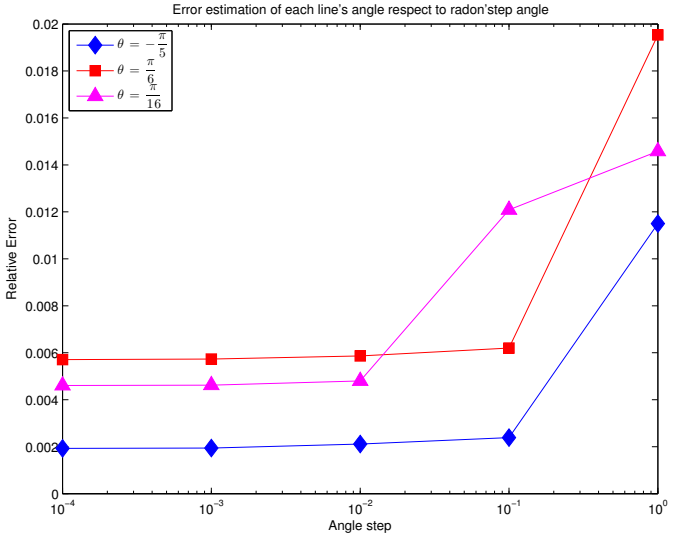

Fig. 5: Variation of the accuracy with respect to the angle step of the Radon transform.